Carbohydrate Polymers 103 (2014) 596–602

Contents lists available at ScienceDirect

Carbohydrate Polymers

journal homepage: www.elsevier.com/locate/carbpol

Acid hydrolysis of native corn starch: Morphology, crystallinity, rheological and thermal properties

R.G. Utrilla-Coello[a,b], C. Hernández-Jaimes[a], H. Carrillo-Navas[a], F. González[a], E. Rodríguez[a], L.A. Bello-Pérez[b], E.J. Vernon-Carter[a], J. Alvarez-Ramirez[a,*]

[a] Universidad Autónoma Metropolitana-Iztapalapa, Departamento de Ingeniería de Procesos e Hidráulica, Apartado Postal 55-534, México, D.F. 09340, Mexico

[b] Centro de Desarrollo de Productos Bióticos (CEPROBI) del Instituto Politécnico Nacional, Yautepec, Morelos, Mexico

ARTICLE INFO

Article history:
Received 11 December 2013
Received in revised form 9 January 2014
Accepted 11 January 2014
Available online 21 January 2014

Keywords:
Corn starch
Acid hydrolysis
Kinetics
Morphology
Crystallinity

ABSTRACT

The acid hydrolysis of native corn starch at 35 °C was monitored during 15 days. After this time, the residual solids were about 37.0 ± 3.0%. First-order kinetics described the hydrolysis data, giving a constant rate of $k_H = 0.18 \pm 0.012$ days^{-1}. Amylose content presented a sharp decrement of about 85% and X-ray diffraction results indicated a gradual increase in crystallinity during the first 3 days. SEM micrographs showed that hydrolysis disrupted granule morphology from an initial regular shape to increasingly irregular shapes. Fractal analysis of SEM images revealed an increase in surface roughness. Fast changes in the thermal effects were caused by molecular rearrangements after fast hydrolysis of amylose in the amorphous regions in the first day. Steady shear rate and oscillatory tests showed a sharp decrease of the apparent viscosity and an increase of the damping factor (tan(δ)) caused by amylose degradation.

1. Introduction

Starch is widely used in the food industry as the main ingredient for the preparation and processing of different products (sausages, bread, pasta, noodles, etc.) or/and as gelling agent, thickener, emulsion stabilizer and fat replacer (Nehir El & Simsek, 2012). Starch is an important determinant of texture, consistency and sensorial acceptance (Björck & Asp, 1994). The structural arrangement of starch components determines the micro-structure of swollen starch granules and amylose/amylopectin ratio, which in turn affect the characteristics of food products (Genovese & Rao, 2003; Lu, Duh, Lin, & Chang, 2008; Ortega-Ojeda, Larsson, & Eliasson, 2004). Acid hydrolysis is widely used in industry for chemical treatment of starch particles (BeMiller & Whistler, 2009). The underlying idea regarding acid hydrolysis is to exploit the susceptibility differences of semi-crystalline and amorphous starch lamellae to acid. Crystalline lamellae were being more resistant to hydrolysis than amorphous lamellae, tending to display negligibly slow hydrolysis while starch amorphous zones were prone to fast acid hydrolysis (Hoover, 2000; Wang, Truong, & Wang, 2003). The degree of crystallinity increased gradually with the time of acid hydrolysis (Wang et al., 2003; Wang, Gao, Yu, & Xiao, 2006). For relatively short hydrolysis times (up to 72 h) acid thinning did not cause disruption of the granular crystalline structure (Singh, Singh Sodhi, & Singh, 2009; Singh Sandhu, Singh, & Lim, 2007). Recent studies indicated that the hydrogen ion primarily attacked firstly the interior and then the exterior of C-type starch granules. B-type starch granules started to crack after about 4 days of hydrolysis, while C-type starch granules cracked until the hydrolysis progressed up to 16 days (Pang et al., 2007). The degradation of amylose and amylopectin by a high acid concentration resulted in a decrease in storage modulus (G′), loss modulus (G″), gelling temperature, and gel strength of acid-thinned starches (Wang et al., 2003). The microstructure of starch granules was strongly disrupted by the action of hydrogen ion, depending on acid concentration and temperature. From an industrial applications standpoint, a close monitoring of the effects of acid hydrolysis on the functionality and micro-structure of starch granules should provide important guidelines for hydrolysis process design oriented to the production of starches with desired functional properties (e.g., crystallinity, shear thinning, etc.).

The aims of this work were: (i) to study the acid hydrolysis of corn starch at 35 °C and to determine the kinetics dynamics of the process; (ii) to monitor the changes in morphology, crystallinity, rheology and particle size with hydrolysis time; (iii) to establish an interrelationship between the progression of these parameters with the hydrolysis kinetics.

* Corresponding author. Tel.: +52 55 5804 4650; fax: +52 55 5804 4650.
E-mail address: jjar@xanum.uam.mx (J. Alvarez-Ramirez).

0144-8617/$ – see front matter © 2014 Elsevier Ltd. All rights reserved.
http://dx.doi.org/10.1016/j.carbpol.2014.01.046

2. Materials and methods

2.1. Materials

Native corn starch was obtained from Gluten y Almidones Industriales, Mexico City, Mexico. H_2So_4 (98%), I_2 (98%) and NaOH (99%) were obtained from J.T. Baker (Mexico City, Mexico). Deionized water was used in all experiments.

2.2. Acid hydrolysis

Acid hydrolysis was carried out according to method reported by Kim, Lee, Kim, Lim, and Lim (2012) with slight modifications. Starch (15 g, dry basis) was dispersed in an aqueous sulphuric acid solution (100 mL, 3.16 M), by stirring and keeping at 35 °C for different time periods (0–15 days). For monitoring the hydrolysis advance, the solution was cooled down to 5 °C for recovering non-hydrolyzed material, including dissolved and suspended starch granules. Afterwards, the suspension was centrifuged (6000 × *g* for 15 min) and the precipitates were washed in distilled water until neutral pH was reached. The precipitated solids were air-dried at 35 °C for 24 h, put into a sealed glass container and stored at 4 °C. In this way, the hydrolysis was monitored as the percent of both suspended solids and dissolved non-hydrolyzed starch relative to the initial starch solids.

2.3. Scanning electron microscopy (SEM)

Native and acid hydrolyzed corn starch particles subjected to different hydrolysis times were mounted on carbon sample holders using double-side sticky tape and were observed using a JEOL JMS 7600F scanning electron microscope (Akishima, Japan) with the GB-H mode at 1 kV accelerating voltage. Micrographs at 3000× magnification are presented.

2.4. Fractal dimension (D_f)

The SEM images were gray leveled as coded images (1000×) on 256 values, 0 (black) to 255 (white) with a resolution of 1280 × 1024 pixels, each pixel being of size of about 3 μm. In order to minimize the anisotropy effects presented by the images, three non-overlapped sample sections of 400 × 400 pixels (1200 μm by side) were taken for each image. For each sample, it was estimated the fractal dimension using the regularization dimension method (Roueff & Véhel, 1998) available at FracLab 2.1 version. The regularization method was chosen for robust computation in the presence of noise contaminated signals. The method consists basically in the estimation of fractal dimension via the behavior of the signal length for increasingly less regularized version of the image. A fractal image exhibits a power law for the lengths as a function of the regularization degree.

2.5. X-ray diffraction (XRD)

Native and acid hydrolyzed corn starch particles subjected to different hydrolysis times were stored in a sealed container at a relative humidity of 85% for achieving constant moisture content. The X-ray powder diffractograms were measured in air at room temperature following the procedure of Hernández-Nava, Bello-Perez, San Martin-Martinez, Hernandez-Sanchez, and Mora-Escobedo (2011) with slight modifications using a Bruker D-8 Advance diffractometer with the Bragg–Brentano θ–θ geometry, Cu Kα radiation, a Ni 0.5% Cu-Kβ filter in the secondary beam, and a one-dimensional position-sensitive silicon strip detector (Bruker, Lynxeye). The diffraction intensity as a function of 2θ angle was measured between 10° and 30°, with a 2θ step of 0.020371°, for 38 s per point.

The crystallinity index was used for quantifying crystallinity changes as function of the hydrolysis time. The crystallinity index, CI_{HW}, was computed with the classical method by Hermans and Weidinger (1948). Briefly, the diffractograms were deconvoluted using Origin 8.0 software and the starch crystallinity index, CI_{HW}, was calculated by the following equation:

$$CI_{HW} = \left(\frac{A_T - A_a}{A_T}\right) \times 100 \quad (1)$$

where A_a is the value of the area under the curve corresponding to the amorphous portion of the diffractograms and A_T is the total area of the diffractograms, i.e., the sum of the areas of all the resulting deconvoluted peaks.

2.6. Amylose content

The apparent amylose content in the aggregate was determined by the Hoover and Ratnayake (2002) test. Starch (20 mg, dry basis) was dissolved in 90% DMSO (8 mL) by using 10-mL screw cap reaction vials. The contents were vigorously mixed for 20 min and then heated in a water bath (with intermittent shaking) at 85 °C for 15 min. The vials were cooled to room temperature (25 °C), and the contents diluted with water to 25 mL in a volumetric flask. The diluted solution (1.0 mL) was mixed with water (40 mL) and mixed with 5 mL I_2/KI solution (2.5 mM I_2 and 6.5 mM KI), adjusting the final volume to 50 mL. The contents were let stand for 15 min at room temperature before measuring the absorbance at 600 nm.

2.7. Differential scanning calorimetry (DSC)

Gelatinization properties of native and acid-modified corn starch particles subjected to different hydrolysis times were analyzed by differential scanning calorimetry (DSC) (TA Instruments, Q1000, New Castle, DE, USA) previously calibrated with indium following the procedure described by Palma-Rodriguez et al. (2012) with slight modifications. A 3.0 mg starch sample (dry basis) was weighed in an aluminum pan 6.0 μL of deionized water was added. Afterwards, the pan was sealed and allowed to equilibrate for 16 h at room temperature before being loaded. The mixture was heated in the DSC cell from 20 to 140 °C applying a heating rate of 5 °C min^{-1}. An empty pan was used as the reference. All measurements were done by triplicate.

2.8. Rheological properties of the starch dispersions

Rheological properties of hydrolyzed starch were determined on starch dispersions, prepared by suspending the starch (15%, w/w) in deionized water. The dispersions were gently stirred and heated at 90 °C for 20 min to allow complete gelatinization of the starch granules. The swollen dispersions were then cooled down and kept in sealed containers. Dynamic oscillatory measurements of the starch dispersions were carried out using a Physica MCR 300 rheometer (Physica Meβtechnik GmbH, Stuttgart, Germany), with a cone–plate geometry, in which the rotating cone was 50 mm in diameter, and cone angle of 2° with a gap of 0.05 mm. About 1.25 mL of sample was carefully placed in the measuring system, and left to rest for 10 min at 25 °C for structure recovery. Amplitude sweeps were carried out in the range of 0.1–1000% at 25 °C. Temperature maintenance was achieved with Physica TEK 150P temperature control and measuring system. The storage modulus (G′) and the loss modulus (G″) were obtained from the equipment software (US200/32 V2.50) in all cases. Flow curves of the starch dispersions were obtained by varying the shear rate from 0.001 to

1000 s^{-1} and the corresponding shear stress and apparent viscosity values measured. Analysis was performed by triplicate.

2.9. Statistical analyses

Data were analyzed using a one way analysis of variance (ANOVA) and a Tukey's test for a statistical significance $P \leq 0.05$, using the SPSS Statistics 19.0. All experiments were done in triplicate.

3. Results and discussion

3.1. Hydrolysis kinetics

The hydrolysis kinetics during 15 days is presented in Fig. 1, expressed in terms of residual unhydrolyzed solids, t. It is apparent that the residual solids exhibited an exponential decaying pattern. In this way, a simple first-order kinetics model of the following form was used for fitting the experimental data:

$$\frac{dR}{dt} = k_H(R_\infty - R) \quad (2)$$

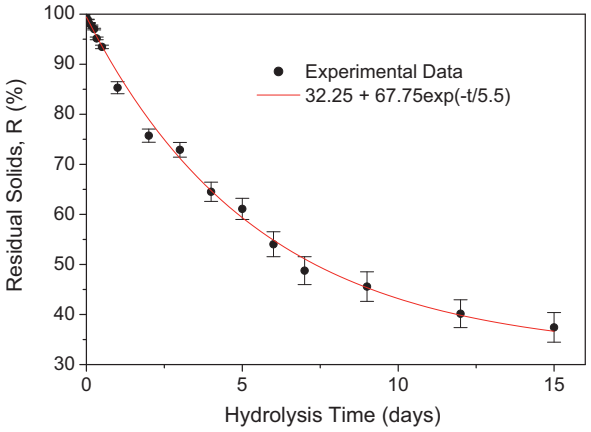

Fig. 1. Starch hydrolysis kinetics during 15 days. The experimental data can be described by a first-order kinetics model.

where R represents the residual solids, k_H is the hydrolysis kinetics constant and R_∞ is the residual solids for very long times. The results are also presented in Fig. 1. The estimated model parameters are $k_H = 0.18 \pm 0.012$ days^{-1} and $R_\infty = 32.25 \pm 2.50\%$.

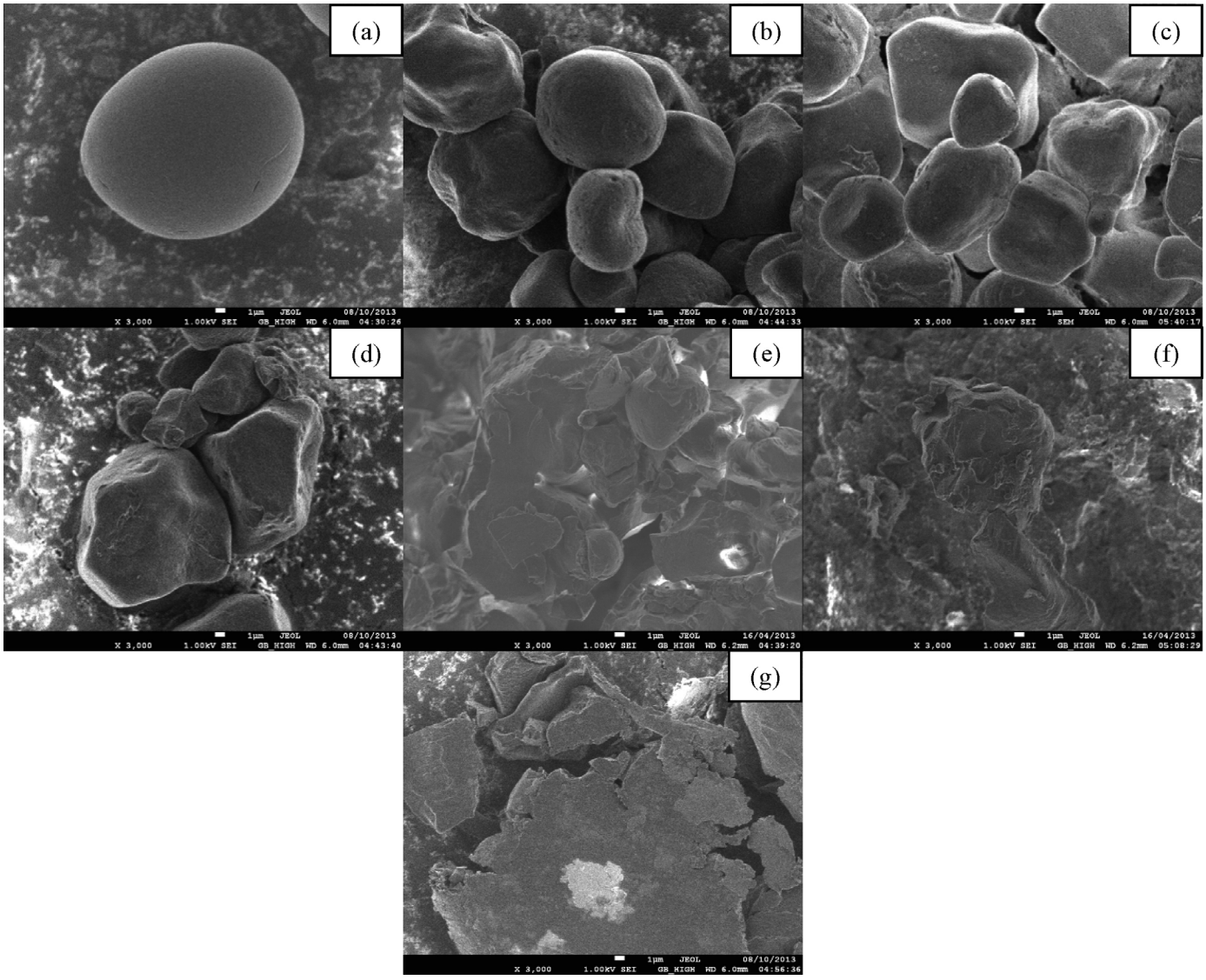

Fig. 2. SEM images of native and hydrolyzed starch particles at different hydrolysis times: (a) native, (b) 12 h, (c) 1 day, (d) 5 days, (e) 7 days, (f) 9 days, (g) 15 days.

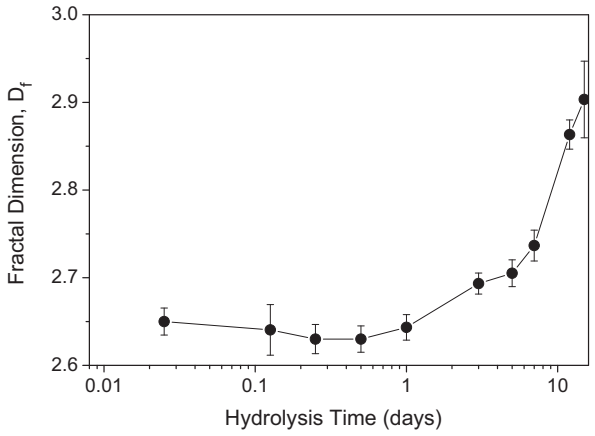

Fig. 3. Regularization fractal dimension as a function of hydrolysis time. Increase of the fractal dimension indicates increase of the surface roughness.

The extent of the corn hydrolysis achieved at day 15 (ca. of $63.0 \pm 3.0\%$) fell short relative to reported conversions of about 85% at 40 °C (Kim et al., 2012). Susceptibility of starches to hydrolysis is strongly affected by temperature as the mobility and activity of the hydrogen ion is largely increased. However, hydrolysis may be also affected by other factors as well, such as the branching location of internal chains, i.e., the clustered versus scattered branching structure (Espinosa-Solis, Sanchez-Ambriz, Hamaker, & Bello-Pérez, 2011; Hoover, 2000).

3.2. SEM study

Native and acid treated starches obtained at different hydrolysis times were observed by SEM (Fig. 2). Native starch granules exhibited a regular, polygonal-like shape with smooth surface. After the first day of hydrolysis, only some starch granule presented slight exo-erosion on the surface, gradually increasing by the third day, but with most of the starch granules maintaining their polygonal shapes. At longer hydrolysis times (5 days and thereafter), deformations on the surface of acid-treated granules were observed. Adhesion between some of the granules (days 5, 7 and 9) and progressive surface erosion and fracture favored by stirring (Le Corre, Bras, & Dufresne, 2011) affected strongly the granule morphology. This pattern became more noticeable at the final stage of the hydrolysis time (15 days). The effect of acid hydrolysis on the granule surface was quantified by computing the regularization fractal dimension D_f (Roueff & Véhel, 1998) based on SEM images of starch granules. The results shown in Fig. 3 indicate that the fractal dimension was nearly constant ($D_f \approx 2.65$) during the first 24 h. Afterwards, the fractal dimension exhibited a gradual increase with hydrolysis time, which is related to an increase of the surface roughness.

3.3. XRD study

XRD patterns of native corn starch and the hydrolyzed fractions at different times are shown in Fig. 4a. Results in Fig. 4a were displayed for this range for better visualization of the intensity peaks characterizing the starch crystallinity. In this way, the dotted vertical lines were used for highlighting four prominent intensity peaks at about 15.0°, 17.0°, 18.0° and 23.0° in 2θ, which were indicative of A-type crystallinity. The peak at 18.0° was much more prominent than the other peaks, and the peak at 23.0° was broader. These intensity peaks appeared in the native and in all of the hydrolyzed fractions. In the first days of hydrolysis, the intensity of the peaks gradually increased, while their width decreased, indicating that

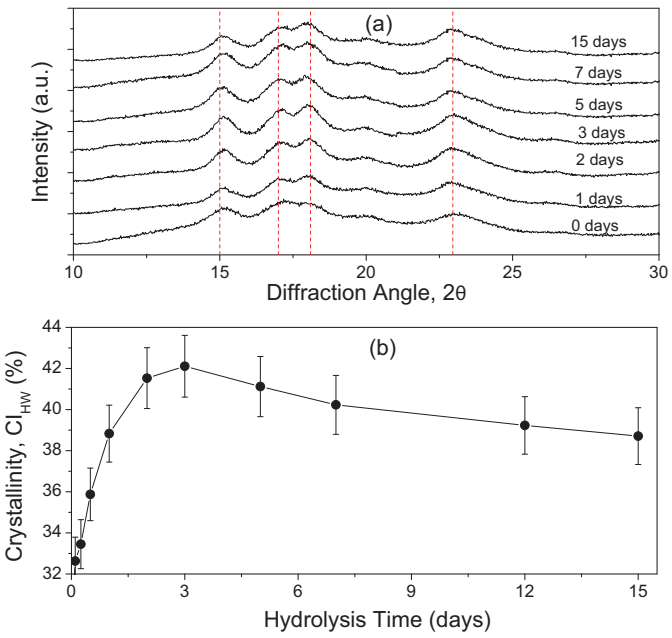

Fig. 4. (a) XRD patterns of native corn starch and the hydrolyzed fractions at different times. Prominent intensity peaks at about 15.0°, 17.0°, 18.0° and 23.0° in 2θ, which are indicative of A-type crystallinity. (b) Evolution of crystallinity index CI_{HW} with the hydrolysis time.

the relative fraction of the crystalline regions increased due to the hydrolysis of the amorphous regions of the starch granules. However, a decrease in the peaks intensity occurred after fifth day. Although crystalline lamellae are more resistant to hydrolysis by chemicals than the amorphous fractions, sulphuric acid disrupted the crystalline structure after the depletion of the rings in the amorphous regions. In principle, this feature should be reflected in the XRD pattern shown in Fig. 4a. Fig. 4b presents the evolution of the crystallinity index with the hydrolysis time. As already observed in Fig. 4b, the crystallinity index CI_{HW} achieved a maximum value (about a 42% increment) after three hydrolysis days. Afterwards, the crystallinity index decreased to achieve values of about 38%. The decreased crystallinity for long hydrolysis times suggests that the acid degraded mainly amylose and long amylopectin chains, leading to an increment in the proportion of less ordered short chains. This corroborates previous findings establishing that, in a first stage, acid hydrolysis affected predominantly the amorphous regions, so that residual starch had more refined crystallinity. The results in Fig. 4b suggest that the crystallinity index can be used as suitable quantities for monitoring the evolution of starch crystallinity during acidic hydrolysis for obtaining, e.g., starch granules with maximum crystallinity content.

3.4. Amylose content

The variation of the amylose content is described in Fig. 5a. A fast decrease occurred during the first 3 days, subsequently achieving a constant value of about 2.94%. The amylose degradation behavior was described by first-order kinetics with mean surviving time-constant of about $\tau_A = 0.85 \pm 0.05$ days. Starch granule swelling allowed amylose leaking from the amorphous regions. Similar to gelatinized starch, once the amylose was in the aqueous phase, it was easily hydrolyzed by hydrogen ions. The residual amylose (about 2.94%) is apparently related to the residual starch resistant to acid hydrolysis. Note the difference between the mean survival time constants between whole starch ($\tau_H = k_H^{-1} = 5.5 \pm 0.35$ days) and amylose fraction ($\tau_A = 0.85 \pm 0.05$ days). This indicates that amylose was hydrolyzed during the first 3 days, while amylopectin

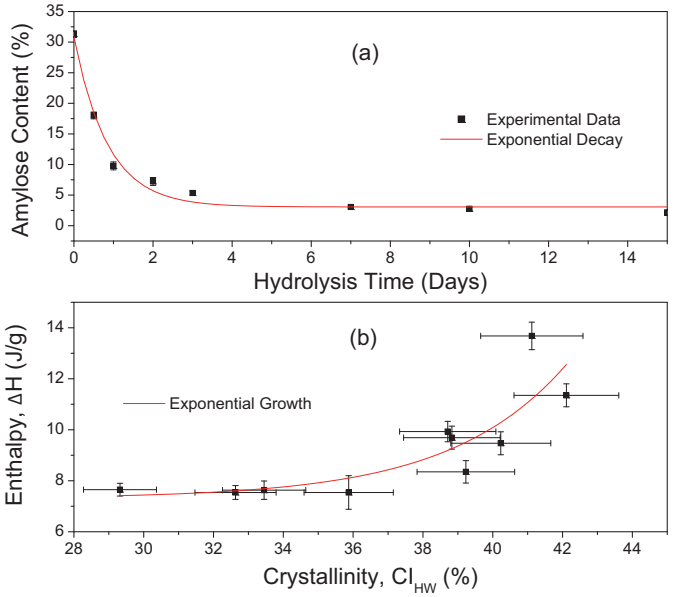

Fig. 5. (a) Variation of the amylose content. A fast decrease is exhibited in the first 3 days. (b) Gelatinization enthalpy ΔH as a function of the crystallinity content CI_{HW}.

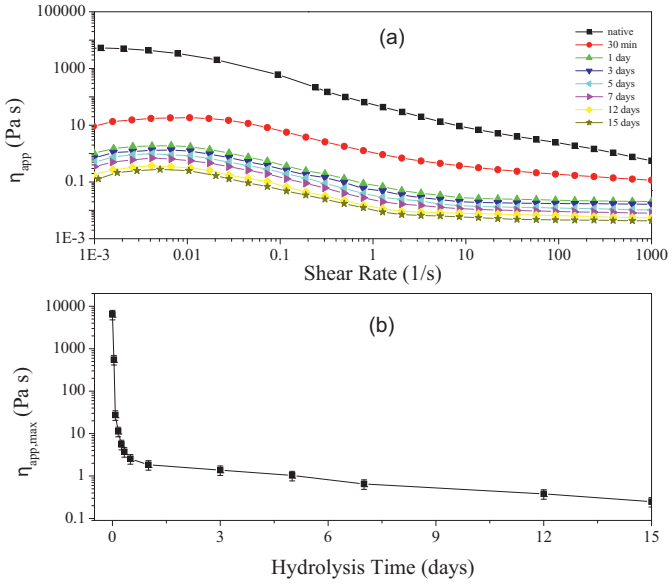

Fig. 6. (a) Constant shear rate viscosity for different values of the hydrolysis time. A shear thinning behavior is observed, with sharp decrease of viscosity after the first hour of hydrolysis.

was more resistant to acid hydrolysis as the latter is located mainly in the semi-crystalline regions of the starch granules. In fact, it is well-known that amylose disrupts the structural order within the amylopectin crystallites (Jenkins & Donald, 1995).

3.5. DSC analysis

The onset, peak, conclusion temperatures (T_o, T_p and T_c), and enthalpy (ΔH) of the phase transition for the native and acid hydrolyzed starches for selected hydrolysis times, are shown in Table 1. The temperatures T_o and T_p decreased and the temperature T_c increased during the first day. The increase in T_c with the acid hydrolysis was related with the removal of the amorphous regions of starch granules, due to the melting of the remaining crystalline regions at higher temperature, but without altering the content and order of the double helices of amylopectin. The gelatinization temperature range T_c–T_o increase in the first hydrolysis day, indicating that the crystallinity heterogeneity was broader for the hydrolyzed granules. The changes in the gelatinization temperatures during the first hydrolysis day coincides with the fast decrement of the amylose content (Fig. 5a), indicating that heterogeneity is linked to the amylose distribution within starch granule structure. In contrast, the gelatinization enthalpy increased to achieve a maximum at the third hydrolysis day to decrease gradually afterwards. It is apparent that the gelatinization enthalpy reflected the average starch crystallinity given by the index CI_{HW} (Fig. 4b). Fig. 5b presents the enthalpy ΔH as a function of the crystallinity content CI_{HW}. A positive correlation between these two parameters was apparent, which can be described as an exponential behavior. In this way, increased starch crystallinity was reflected as increased gelatinization enthalpy, so that high crystallinity values were also related to improvements in the order of amylopectin molecules within the double helices arrangement.

3.6. Starch dispersions apparent viscosity

The apparent viscosity-shear rate behavior of the starch dispersions subjected to different hydrolysis times is presented in Fig. 6a. All the starch dispersions showed typical behavior of flocculated dispersions. Flocculated dispersions exhibit pronounced shear thinning behavior due to two main factors: (1) the flocs are deformed and become aligned with the shear field, which decreases their resistance to flow, and (2) the flocs are disrupted by shear forces, which decreases their effective volume fraction (McClements, 2005). A dispersion containing flocculated solids tends to show a higher apparent viscosity than one than contains the same concentration of unflocculated solids. This is because the effective volume fraction of a floc is greater than the sum of volume fractions of the individual solids due to the presence of the continuous phase trapped within it (Dickinson & Stainsby, 1982). The rate at which the flocs in dispersions are deformed and disrupted decreases as the number and the strength of the attractive interactions between solids increases. Thus it may be inferred from the curves in Fig. 6a that the native corn starch dispersion had a higher effective volume fraction and attained stronger interaction forces than the hydrolyzed starch dispersions. As hydrolysis time proceeded, and residual solids decayed, the effective volume fraction of the hydrolyzed starch dispersions decreased, and the apparent viscosity decreased. Fig. 6b depicts the drop in maximum apparent viscosity as a function of hydrolysis time. The decrease in apparent viscosity was of about 99.9% in the first 12 h, and is in line with the decrease of the amylose content (Fig. 5a). In fact, gelatinized amylose is the main contributor to the viscosity in starch dispersions. In particular, the reduction of short-chain amylose affects largely the viscosity of starch dispersions (Zhang, Zhu, Shao, Gu, & Liu, 2012). In this way, it may be argued that the residual amylose content (Fig. 5a) is not leaked within the aqueous phase, but is contained within the intrinsic crystalline structure. In turn, this makes the residual amylose resistant to acid hydrolysis.

3.7. Viscoelasticity of starch dispersions

Fig. 7a and b presents the storage G′ and the loss G″ modulus as a function of the applied strain. For all hydrolysis times, the storage modulus G′ exhibited a monotonous decreasing behavior with the applied strain, indicating that the elasticity of the starch dispersions was reduced under shear action. For very short hydrolysis times (up to about 1 h), the loss modulus G″ exhibited a Newtonian region for small strains and a small overshoot in the region of about 20–60% strain. Following the classification of complex fluids (Hyun, Kim,

Table 1
Thermal parameters of native and hydrolyzed corn starch at different hydrolysis times.

Time	T_o (°C)	T_p (°C)	T_c (°C)	ΔH (J/g)	T_c–T_o (°C)
Native	57.73 ± 0.72^{b,c}	72.16 ± 0.26^{e}	81.13 ± 0.92^{a}	7.65 ± 0.31^{a}	22.91 ± 0.25^{a}
0.5 d	58.03 ± 0.82^{c}	71.59 ± 0.38^{d,e}	82.99 ± 1.10^{a}	7.54 ± 0.31^{a}	24.96 ± 0.28^{a}
1 d	49.89 ± 0.63^{a}	65.24 ± 0.59^{a}	94.69 ± 0.53^{b,c}	9.69 ± 0.66^{b}	44.80 ± 1.17^{c,d}
3 d	51.88 ± 0.02^{a}	70.37 ± 0.10^{c,d}	98.58 ± 0.08^{d}	11.35 ± 0.08^{c}	46.69 ± 0.05^{d}
5 d	50.48 ± 2.28^{a}	66.91 ± 0.76^{b}	95.58 ± 0.00^{c}	13.68 ± 0.36^{d}	45.09 ± 2.28^{c,d}
7 d	51.26 ± 1.05^{a}	67.11 ± 0.16^{b}	93.25 ± 0.56^{b}	9.47 ± 0.00^{b}	41.99 ± 1.61^{b,c}
12 d	55.52 ± 0.49^{b,c}	70.15 ± 0.60^{c}	95.21 ± 0.73^{b,c}	7.35 ± 0.45^{a}	39.69 ± 0.24^{b}
15 d	55.00 ± 0.91^{b}	74.63 ± 0.25^{f}	102.03 ± 1.00^{e}	9.93 ± 0.40^{b}	47.03 ± 1.91^{d}

Values are means ± standard error, of three replicates.
Superscripts with different letters in same column indicate significant differences ($P \leq 0.05$).
d = days; T_o, T_p, and T_c = onset, peak, and conclusion temperatures; ΔH = enthalpy change, T_c–T_o = gelatinization temperature range.

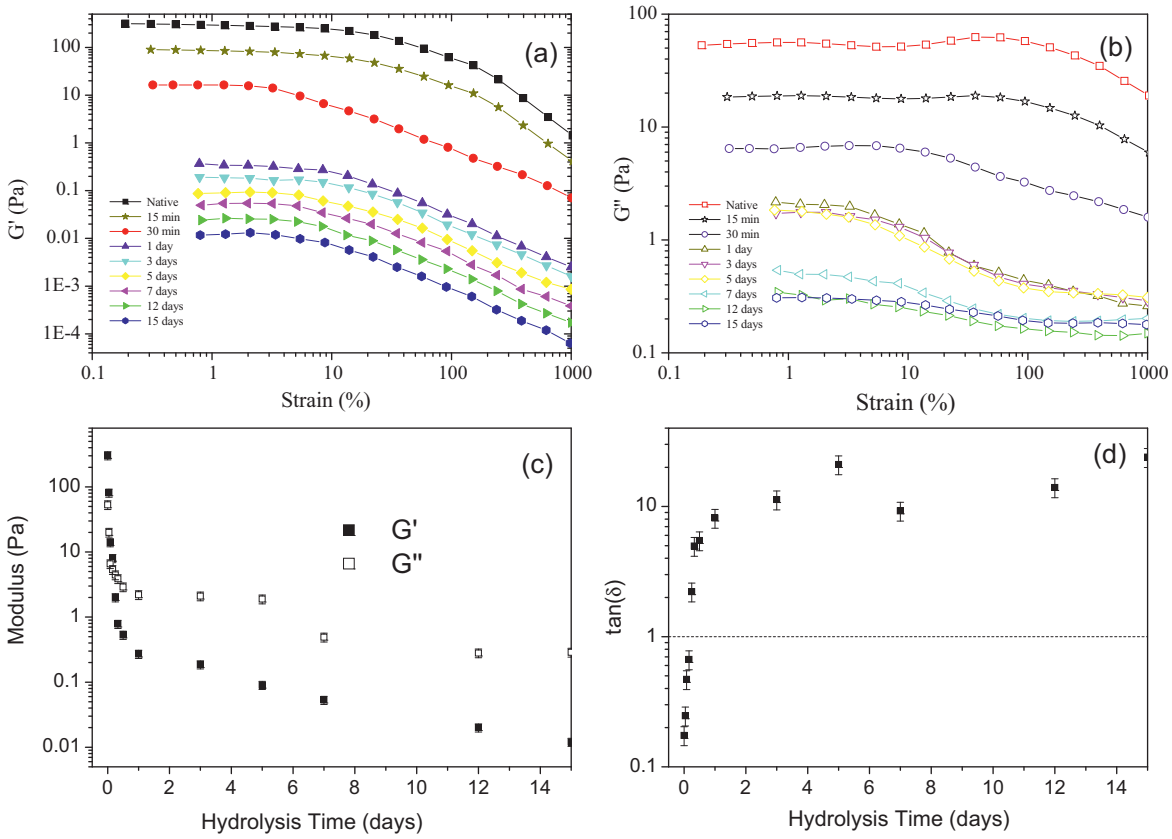

Fig. 7. (a) Storage G′ and (b) loss G″ moduli as a function of the applied strain. An overshoot in the loss modulus is observed for native weakly hydrolyzed corn starch dispersions. (c) Decrease of the complex modulus as a function of the hydrolysis time. (d) Damping factor tan(δ), showing the loss of viscoelasticity with hydrolysis time.

Ahn, & Lee, 2002), starch dispersions were characterized by Type III microstructure. The overshoot of the loss modulus was caused by molecule shear-induced aggregation, forming a weakly structured material. This complex structure was destroyed by the application of large deformations over the critical strain, after which the biomolecules chains aligned with the flow field and the loss modulus decreased. However, the loss modulus overshoot disappeared after 1 h of hydrolysis time. The dispersions aggregates responsible of the loss modulus overshoot were induced by gelatinized amylose molecules. Starch granules with low amylose content produced weak gels (shear thinning) for all strain range after the first hour of hydrolysis.

For 1% of strain, Fig. 7c presents the complex modulus G′ and G″ as a function of the hydrolysis time. Both moduli decreased sharply in the first hydrolysis hours, reflecting the depletion of amylose content. The corresponding damping factor $\tan(\delta) = G''/G'$, an index of the gel fluidization, is presented in Fig. 7d. After the first hour, the damping factor $\tan(\delta) > 1$, indicating that the starch dispersions had a liquid-like behavior (Wang et al., 2003). This shows that important viscoelasticity reductions for starch dispersions were obtained with relatively short hydrolysis times of the order of 1 h.

4. Conclusions

In this work a detailed characterization of acid hydrolysis of native corn starch for short and long time horizons is given. Different techniques were used to this end, including XRD, DSC, amylose content determination, fractal analysis of SEM images and rheology of starch dispersions. Results showed that amylose content played an important role in the hydrolyzed starch characteristics for short time scales. In contrast, disruption of the starch granule integrity was determinant in the long term, affecting mainly crystallinity and thermal properties. The results showed that hydrolysis is a flexible process for starch treatment under desired characteristics. In this way, the production of shear thinning starch with relatively

low hydrolysis advance required only few hours. In contrast, the production of starch granules with high crystallinity required moderate hydrolysis advance and longer times of the order of 2–3 days. Overall, the results in this work showed that acid hydrolysis is a complex process underlying starch microstructure changes in time scales from hours to days.

Acknowledgements

The authors want to thank CONACyT-México for providing financial support under project INFR-2011-1-163250. Also, special thanks to LDRX (T-128) UAM-I for XRD measurements.

References

BeMiller, J. N., & Whistler, R. L. (2009). *Starch: Chemistry and technology* (3rd ed.). New York: Elsevier.

Björck, I., & Asp, N. G. (1994). Controlling the nutritional properties of starch in foods – A challenge to the food industry. *Trends in Food Science and Technology*, *5*(7), 213–218.

Dickinson, E., & Stainsby, G. (1982). *Colloids in foods*. London: Applied Science Publishers.

Espinosa-Solis, V., Sanchez-Ambriz, S. L., Hamaker, B. R., & Bello-Perez, L. A. (2011). Fine structural characteristics related to digestion properties of acid-treated fruit starches. *Starch/Stärke*, *63*, 717–727.

Genovese, D. B., & Rao, M. A. (2003). Role of starch granule characteristics (volume fraction, rigidity, and fractal dimension) on rheology of starch dispersions with and without amylose. *Cereal Chemistry*, *80*, 350–355.

Hermans, P. H., & Weidinger, A. (1948). Quantitative X-ray investigations on the crystallinity of cellulose fibers. A background analysis. *Journal of Applied Physics*, *19*, 491–506.

Hernández-Nava, R. G., Bello-Pérez, L. A., San Martín-Martínez, E., Hernández-Sánchez, H., & Mora-Escobedo, R. (2011). Effect of extrusion cooking on the functional properties and starch components of lentil/banana blends: Response surface analysis. *Revista Mexicana de Ingeniería Química*, *10*, 409–419.

Hoover, R. (2000). Acid-treated starches. *Food Reviews International*, *16*, 369–392.

Hoover, R., & Ratnayake, W. S. (2002). Starch characteristics of black bean, chick pea, lentil, navy bean and pinto bean cultivars grown in Canada. *Food Chemistry*, *78*, 489–498.

Hyun, K., Kim, S. H., Ahn, K. H., & Lee, S. J. (2002). Large amplitude oscillatory shear as a way to classify the complex fluids. *Journal of Non-Newtonian Fluid Mechanics*, *107*, 51–65.

Jenkins, P. J., & Donald, A. M. (1995). The influence of amylose on starch granule structure. *International Journal of Biological Macromolecules*, *17*, 315–321.

Kim, H. Y., Lee, J. H., Kim, J. Y., Lim, W. J., & Lim, S. T. (2012). Characterization of nanoparticles prepared by acid hydrolysis of various starches. *Starch/Stärke*, *64*, 367–373.

Le Corrre, D., Bras, J., & Dufresne, A. (2011). Evidence of micro- and nanoscaled particles during starch nanocrystals preparation and their isolation. *Biomacromolecules*, *12*, 3039–3046.

Lu, T. J., Duh, C. S., Lin, J. H., & Chang, Y. H. (2008). Effect of granular characteristics on the viscoelastic properties of composites of amylose and waxy starches. *Food Hydrocolloids*, *22*, 164–173.

McClements, D. J. (2005). *Food emulsions: Principles, practices, and techniques* (2nd ed.). Florida: CRC Press.

Nehir El, S., & Simsek, S. (2012). Food technological applications for optimal nutrition: An overview of opportunities for the food industry. *Comprehensive Reviews in Food Science and Food Safety*, *11*, 2–12.

Ortega-Ojeda, F. E., Larsson, H., & Eliasson, A. C. (2004). Gel formation in mixtures of high amylopectin potato starch and potato starch. *Carbohydrate Polymers*, *56*, 505–514.

Palma-Rodriguez, H. M., Agama-Acevedo, E., Mendez-Montealvo, G., Gonzalez-Soto, R. A., Vernon-Carter, E. J., & Bello-Pérez, L. A. (2012). Effect of acid treatment on the physicochemical and structural characteristics of starches from different botanical sources. *Starch/Stärke*, *64*, 115–125.

Pang, J., Wang, S., Yu, J., Liu, H., Yu, J., & Gao, W. (2007). Comparative studies on morphological and crystalline properties of B-type and C-type starches by acid hydrolysis. *Food Chemistry*, *105*, 989–995.

Roueff, F., & Véhel, J. L. (1998). A regularization approach to fractional dimension estimation. *Fractals*, *98*, 1–13.

Singh, H., Singh Sodhi, N., & Singh, N. (2009). Structure and functional properties of acid thinned sorghum starch. *International Journal of Food Properties*, *12*, 713–725.

Singh Sandhu, K., Singh, N., & Lim, S. T. (2007). A comparison of native and acid thinned normal and waxy corn starches: Physicochemical, thermal, morphological and pasting properties. *LWT – Food Science and Technology*, *40*, 1527–1536.

Wang, Y. J., Truong, V. D., & Wang, L. (2003). Structures and rheological properties of corn starch as affected by acid hydrolysis. *Carbohydrate Polymers*, *52*, 327–333.

Wang, S. J., Gao, W. Y., Yu, J. L., & Xiao, P. G. (2006). The crystalline changes of starch from Rhizoma Dioscorea by acid hydrolysis. *Chinese Chemical Letters*, *17*, 1255–1258.

Zhang, C., Zhu, L., Shao, K., Gu, M., & Liu, Q. (2012). Toward underlying reasons for rice starches having low viscosity and high amylose: Physiochemical and structural characteristics. *Journal of the Science of Food and Agriculture*, *93*, 1543–1551.